Signal processing methods for Coriolis Mass Flow Metering in two-phase flow conditions

Ming Li and Manus Henry

Original citation & hyperlink:
Li, M. and Henry, M., 2016, March. Signal processing methods for Coriolis Mass Flow Metering in two-phase flow conditions. In *2016 IEEE International Conference on Industrial Technology (ICIT)* (pp. 690-695). IEEE.
https://dx.doi.org/10.1109/ICIT.2016.7474833

DOI 10.1109/ICIT.2016.7474833
Publisher: IEEE

Signal Processing Methods for Coriolis Mass Flow Metering in Two-Phase Flow Conditions

Ming Li, Manus Henry
Department of Engineering Science
University of Oxford
Oxford, OX1 3PJ, UK.
manus.henry@eng.ox.ac.uk

Abstract— **Improved signal processing methods for Coriolis Mass Flow Meters provide more accurate measurements and offer a wider range of applications, such as two-phase flow. This paper reviews current signal processing methods for amplitude, frequency and phase difference tracking and analyses their performance in a simulation of two-phase flow conditions.**

Keywords—Coriolis Mass Flow Meter, signal processing, dynamic response, time delay, frequency tracking, phase difference tracking, amplitude tracking.

I. INTRODUCTION

The Coriolis Mass Flow (CMF) meter, has undergone significant development over the last 20 years [1]. The meter consists of a vibrating flowtube in series with the process piping, and an electronic transmitter that maintains flowtube vibration, performs measurement calculations, and transmits measurement data [2]. The frequency of oscillation (typically 50 Hz - 1 kHz for different flow-tube designs) indicates the density of the process fluid, while the phase difference between the sensor signals indicates the mass flow rate [3]. CMF meters provide high accuracy (e.g. 0.1% of reading for steady flow rates) and good turndown (e.g. 100:1). As digital techniques have developed, the CMF meter has migrated from analogue to digital implementations. Signal processing techniques have evolved to track the amplitude, frequency and phase of the sensor signals for measurement, and to generate a drive signal to maintain flow tube oscillation. Some have suggested the CMF meter is an "almost perfect" flowmeter [4], but limitations have included an inability to maintain flowtube oscillation and/or provide accurate measurements when presented with mixtures of gas and liquid.

Signal processing methods for single phase (i.e. pure gas or liquid) measurement are well established. Techniques in the recent literature [1], [5], [6] include Fourier Transform, Digital Phase Locked Loop, Digital Correlation, Adaptive Notch Filter, and the Hilbert Transform. Two methods not considered are the Sliding Goertzel Algorithm (SGA) [7] and Quadrature Demodulation (QD) [8]. Both have inherent limitations relating to dynamic response that prevent further consideration here.

The dynamic response [9]–[12] of the CMF meter is a significant issue in two application areas. Conventionally, the response of the meter is important for batching applications such as small volume proving, where industrial standards are based on the response time of mechanical meters [13]. More recently, for CMF meters capable of operating in two-phase or three-phase flow [14], tracking of the rapidly varying amplitude, frequency and phase of the sensor signals is important in order to generate an optimal drive signal [3]. For example, figure 1.1 shows typical sensor signals observed when the flowtube is filled with a single-phase fluid. The amplitude and frequency of the sensor signals are steady.

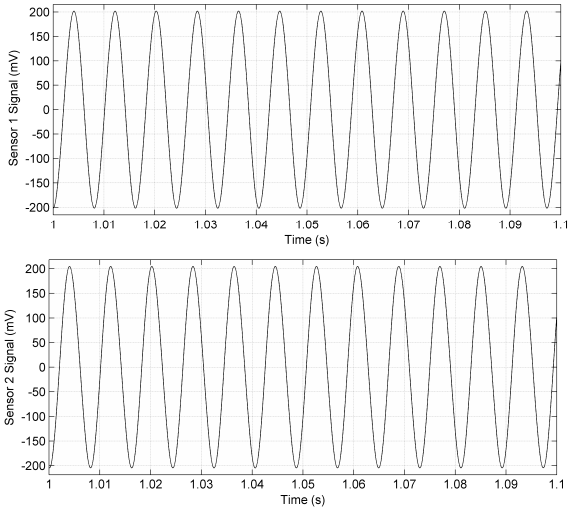

Fig. 1.1: Sensor signals during steady single phase flow

By contrast, figure 1.2 shows typical sensor signals with a mixture of liquid and gas. Changes in the distribution of liquid and gas in the flowtube lead to variable damping, and rapid changes in the frequency and amplitude of oscillation. The challenge to the amplitude control system is significant, and a fast dynamic response for the measurement of frequency, phase and amplitude should lead to improved flowtube control, as well as measurement, in the presence of two-phase flow.

The purpose of this paper is to evaluate the ability of various signal processing approaches to track rapid changes in the sensor signal properties. With the increasing importance of two-phase flow, this analysis includes the tracking of variable amplitude (often neglected in the prior literature) alongside the calculation of phase difference and frequency.

This research was carried out with the support of Schneider Electric

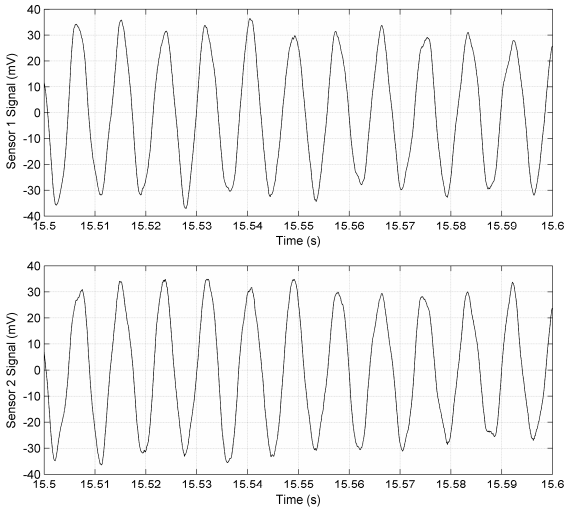

Fig. 1.2: Sensor signals during two-phase flow

II. METHOD ANALYSIS

A. Discrete Fourier Transform

A well-established approach for tracking the frequency of a sinusoid is to calculate the signal's Fourier coefficients and map the results into the frequency domain. The peak in the frequency domain gives the best estimate of the signal's frequency. Phase difference can be calculated using the Discrete Time Fourier Transform (DTFT) based on the peak frequency. For efficient real-time implementation and/or to reduce spectral leakage, windowing techniques (e.g. rectangular, Hanning) may be applied. Rectangular windowing can be implemented via a recursive calculation to reduce the computational load, while other windowing techniques can reduce spectral leakage.

For rectangular windowing, DFT values at time n can be calculated recursively from the results at time n-1, using

$$DFT_R(n,k) = [x(n+N/2-1) - x(n-N/2-1)](-1)^k e^{j2\pi k/N} + DFT_R(n-1,k)e^{j2\pi k/N} \quad (1)$$

Here $x(t)$ is the input signal function, N is the window length and $k=0,1,\cdots,N/2-1$. In [15], Hirokazu et at al. applied the DFT method to track the frequency of a Coriolis flowtube in a commercial implementation.

Once the current frequency has been determined, the phase difference and amplitude can be calculated using the Discrete Time Fourier Transform (DTFT), based on the tracked frequency's Fourier coefficients. Tu et al. [16] explored the spectral leakage problem and determined the phase of a periodic signal from an arbitrary number of samples without spectral leakage by considering the negative frequency contribution. Shen et al. [17] further improved the recursive DTFT algorithm and increased the accuracy of the phase difference tracking. The equation for their most recent recursive DTFT algorithm is as follows:

$$\begin{aligned} X_{m,N}(\hat{\omega}_m) &= \sum_{n=0}^{N-1} x(m+n)\cdot e^{-j\hat{\omega}_m n} \\ &= x(m) + x(m+1)\cdot e^{-j\hat{\omega}_m} + x(m+2)\cdot e^{-2j\hat{\omega}_m} \\ &\quad + \cdots + x(m+N-1)\cdot e^{-j\hat{\omega}_m(N-1)} \end{aligned} \quad (2)$$

At the next sample time $m+1$, this becomes:

$$\begin{aligned} X_{m+1,N}(\hat{\omega}_{m+1}) &= \sum_{n=0}^{N-1} x(m+1+n)\cdot e^{-j\hat{\omega}_{m+1}n} \\ &= \left[\sum_{n=0}^{N-1} x(m+n)\cdot e^{-j\hat{\omega}_{m+1}n} - x(m)\right]\cdot e^{-j\hat{\omega}_{m+1}} \\ &\quad + x(m+N)\cdot e^{-j\hat{\omega}_{m+1}(N-1)} \\ &\approx \left[\sum_{n=0}^{N-1} x(m+n)\cdot e^{-j\hat{\omega}_m n} - x(m)\right]\cdot e^{-j\hat{\omega}_{m+1}} \\ &\quad + x(m+N)\cdot e^{-j\hat{\omega}_{m+1}(N-1)} \\ &= [X_{m,N}(\hat{\omega}_m) - x(m) + x(m+N)\cdot \\ &\quad e^{-j\hat{\omega}_{m+1}N}]\cdot e^{-j\hat{\omega}_{m+1}} \end{aligned} \quad (3)$$

In (2) and (3), $\hat{\omega}_m$ and $\hat{\omega}_{m+1}$ represent the estimated frequencies for the two adjacent sampling points.

To a limited extent, the DFT can overcome the interference of harmonics and noise, is operationally efficient, and is easy to implement in real-time hardware. However, the FFT has inherent performance limitations, such as spectral leakage and the picket fence effect, due to nonsynchronous sampling [18]. Also there is an unavoidable trade-off between time and frequency domain resolution, based on the window length. In two-phase flow situations, the sensor signal varies rapidly, so the measurement needs a fast dynamic response. This requires high time domain resolution which, for the DFT method, will result in decreased frequency domain resolution. Hence the DFT method cannot guarantee high frequency resolution for two-phase flow situations.

For phase difference tracking, the negative frequency-based DTFT algorithm improves the precision but spectral leakage problems still exist with nonsynchronous sampling. Other methods ([19], [20]) have reduced the phase difference error using Rectangular Self-Convolution Windows (RSCWs) but the resulting dynamic response has not been explored.

B. Digital Phase Locked Loop

Freeman [21] used a Digital Phase Locked Loop (DPLL) to track frequency and phase difference for a CMF meter. As shown in Figure 2.1, the signals are multiplied by a modulation function $c(n) = \exp(-j2\pi f_h nt)$, where f_h is close to the sensor signal frequency, so that the resulting product is shifted close to zero hertz (DC). Comb filters are used to remove harmonic noise, followed by decimation and down-sampling. Three FIR filters track the down-sampled signals at frequencies $-f_h/16$, 0 and $+f_h/16$ with linear or quadratic interpolation providing a final estimate of the flowtube resonant frequency.

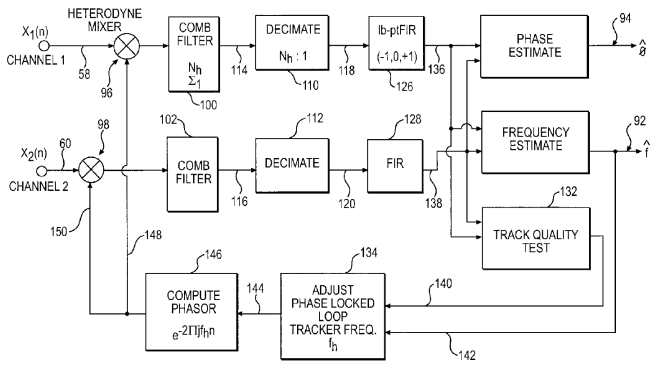

Fig.2.1. Digital Phase Locked Loop diagram [21]

C. *Adaptive Notch Filters*

There have been many academic and commercial applications of ANFs to CMF meter frequency tracking, with perhaps the first example described by Derby et al.[22]. Performance improvements are obtained by adopting the Steiglitz-McBride ANF (SMM-ANF) [7], [23]. Typically, a DTFT technique is used to complete the calculation of phase difference and amplitude. Figure 2.2 shows the structure of SMM-ANF algorithm:

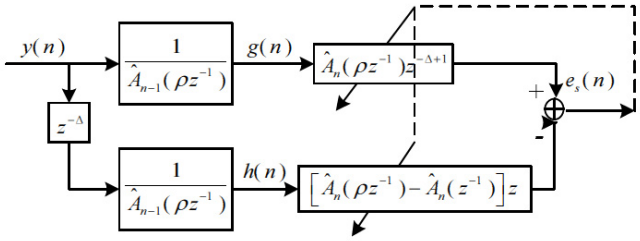

Fig. 2.2: Structrue of SMM-ANF [7]

Here the transform function is:

$$H(z)=\frac{\hat{A}_n(z^{-1})}{\hat{A}_n(\rho z^{-1})}=\prod_{k=1}^{m}\frac{1+\hat{\alpha}_k(n)z^{-1}+z^{-2}}{1+\rho_k(n)\hat{\alpha}_k(n)z^{-1}+\rho_k^2(n)z^{-2}} \quad (4)$$

where m *is* the trap number i.e. the number of peak frequencies to be tracked. Since the CMF signal has a single dominant frequency, m=1. $\rho_k(n)$ is the pole contraction factor which determines the bandwidth of the ANF, given by:

$$BW=2\cos^{-1}\left(\frac{2\rho_k(n)}{1+\rho_k^2(n)}\right) \quad (5)$$

The bandwidth is initially broad to capture the frequency of the input signal and is then narrowed to achieve convergence and improved accuracy. Hence $\rho_k(n)$ is increased over time [24]:

$$\rho_k(n)=\rho_0\rho_k(n-1)+(1-\rho_0)\rho_\infty \quad (6)$$

The weight coefficient $\hat{\alpha}_k(n)=-2\cos\hat{\omega}_k(n)$, with $\hat{\omega}_k(n)$ the notch frequency estimate of the input frequency, is adjusted by a Recursive Mean Square (RMS) algorithm:

$$\hat{\alpha}_k(n+1)=\hat{\alpha}_k(n)-P(n)\psi(n)e_s(n) \quad (7)$$

where $\psi(n)$ is the gradient function, $P(n)$ represents the covariance parameters, $\lambda(n)$ is the forgetting factor, and $e_s(n)$ represents the output of ANF shown in Figure 2.2.:

$$\psi(n)=\frac{\partial e_s(n)}{\partial\hat{\alpha}_k(n)}=\frac{y(n-1)-\rho_k(n)e_s(n-1)}{1+\rho_k(n)\hat{\alpha}_k(n)z^{-1}+\rho_k^2(n)z^{-2}} \quad (8)$$

$$P(n)=\frac{(1-\lambda(n))P(n-1)}{\lambda(n)+\psi^2(n)P(n-1)} \quad (9)$$

$$\lambda(n)=\lambda_0\lambda(n-1)+(1-\lambda_0)\lambda_\infty \quad (10)$$

When implementing the SMM-ANF algorithm in the simulation described below, the initial values are:

$$\begin{aligned}&f_s=2kHz,\rho(1)=\rho(2)=\rho_0=0.9,\rho_\infty=0.995,\\&P(1)=P(2)=100,\lambda(1)=\lambda(2)=\lambda_0=0.9,\lambda_\infty=0.995\end{aligned} \quad (11)$$

There are limitations on how well this technique can track signals with rapidly changing amplitude, as occurs in two-phase flow. Recently, Yin et al.[25] developed the Amplitude Adaptive Notch Filter (AANF) to enable the method to work with an amplitude varying signal. However, AANF was designed for Grid Signal Processing, and the application of AANF in CMF signal processing remains unexplored.

D. *Digital Correlation*

Wray et al. [26] describe a correlation method for finding the phase difference α between sensor signals, A and B. Given:

$$A=a\sin\omega t \quad (12)$$

$$B=b\sin(\omega t+\alpha) \quad (13)$$

Then the cross product $A\otimes B$ can be written as:

$$A\otimes B=ab\int_0^{2\pi}\sin\omega t\sin(\omega t+\alpha)dt \quad (14)$$

Thus the phase difference can be represented as:

$$\alpha=2\times\frac{A\otimes B}{ab} \quad (15)$$

Further techniques are required to track frequency and amplitude. Although this technique was originally developed for analogue signal processing, Ruoff et al. [5] discuss its merits in the context of digital processing.

E. *Hilbert Transform*

Duffill et al. [27] applied the Hilbert transform to form an analytic signal for CMF tracking. FIR Hilbert filtering of the sensor signals creates Hilbert pairs. The original left and right pickoff (i.e. sensor) input signals are defined as:

$$LPO_{ori}=A_{lpo}\cos(wt+\theta/2) \quad (16)$$

$$RPO_{ori}=A_{rpo}\cos(wt-\theta/2) \quad (17)$$

where θ is the phase difference and w is the frequency in radians per second. The Hilbert filtered signals are combined with the original sensor signals to yield:

$$\begin{aligned} LPO &= A_{lpo}[\cos(wt-\theta/2)+j\sin(wt-\theta/2)] \\ &= A_{lpo}e^{j(wt-\theta/2)} \end{aligned} \tag{18}$$

with the equivalent calculation for RPO. Taking the conjugate of the left input Hilbert pairs and multiplying by the right input Hilbert pairs yields the following equation:

$$\begin{aligned} \overline{LPO}\times RPO &= A_{lpo}e^{-j(wt-\theta/2)}\times A_{rpo}e^{j(wt+\theta/2)} \\ &= A_{lpo}\times A_{rpo}e^{j\theta} \end{aligned} \tag{19}$$

Assuming the left and right sensor signals have equal amplitude simplifies this to:

$$\overline{LPO}\times RPO = A^2(\cos\theta + j\sin\theta) \tag{20}$$

The phase difference can be obtained using:

$$\theta = \arg(\overline{LPO}\times RPO) \tag{21}$$

The amplitude is calculated from the Hilbert pairs:

$$A_{lpo} = A_{rpo} = abs(LPO) = abs(RPO) \tag{22}$$

The frequency is obtained based on the phase change between successive samples:

$$\begin{aligned} \overline{LPO}_{n-1}\times LPO_n &= A_{lpo}e^{-j(wt_{n-1}-\theta/2)}\times A_{lpo}e^{j(wt_n-\theta/2)} \\ &= A_{lpo}^2 e^{j(wt_n-wt_{n-1})} \end{aligned} \tag{23}$$

The frequency (in radians) of the left input signal is given by:

$$wt_n - wt_{n-1} = \arg(\overline{LPO}_{n-1}\times LPO_n) \tag{24}$$

Converting into Hz:

$$f_{lpo} = \frac{(wt_n - wt_{n-1})\times Fs}{2\pi} \tag{25}$$

where Fs is the sampling rate of the input signal. Peng et al. [6] claim the Hilbert transform is not suitable for frequency tracking, while Tu et al. [7] use ANF for frequency tracking, and the Hilbert transform for phase difference calculation. However, as shown in the equations above and the results below, the Hilbert technique can be adapted to track frequency, amplitude and phase difference simultaneously.

III. SIMULATION RESULTS

Previous authors have not discussed the most effective signal processing technique for dealing with mixtures of liquid and gas. The main challenge here is the dynamic response of the signal processing algorithm to deal with rapid and simultaneous changes in amplitude, frequency and phase difference. The importance of fast dynamic response for single phase applications has been thoroughly discussed in [9]–[12].

The authors have developed a set of benchmark simulations to evaluate CMF signal processing techniques against a range of scenarios, entailing linear, sinusoidal and/or random changes in amplitude, frequency and/or phase difference, where such parameter changes may occur singly or in combination. These benchmarks are based on our extensive experience of using CMF meters in two-phase and three-phase applications [14]. The full of benchmark tests will be discussed in future journal papers. Here, only a single test is discussed, which extends an example previously described in the literature [7].

Three of the methods described above have been implemented in simulation, and applied to sensor signals with randomly varying amplitude, frequency and phase difference. The standard deviation of the error for each parameter value has been calculated, and the results compared for each method. Time-varying sensor signals are generated using an amended version of the random walk model from [7], as follows:

$$\begin{aligned} y_1(n) &= A(n)\sin[2\pi n f(n)/f_s + \phi(n)/2] + \sigma_{e1}\cdot e_1(n) \\ y_2(n) &= A(n)\sin[2\pi n f(n)/f_s - \phi(n)/2] + \sigma_{e2}\cdot e_2(n) \\ A(n) &= A(n-1) + \sigma_A \cdot e_A(n) \\ f(n) &= f(n-1) + \sigma_f \cdot e_f(n) \\ \phi(n) &= \phi(n-1) + \sigma_\phi \cdot e_\phi(n) \end{aligned} \tag{26}$$

Here y_1 and y_2 are the simulated sensor signals, with common but time varying amplitude A, frequency f, and phase difference ϕ. The sampling update rate for the simulation, f_s, is 2 kHz. $e_1(n)$, $e_2(n)$, $e_A(n)$, $e_f(n)$ and $e_\phi(n)$ are un-correlated white noise processes, which, like using a common amplitude for the two sensor signals, represents a simplification of actual two phase flow conditions. With two-phase flow there is likely to be some correlation between the true mass flow and density values – for example, when a slug of liquid passes through the flowtube both parameter values should increase together. σ_{e1}, σ_{e2}, σ_A, σ_f and σ_ϕ are multiplying factors for the random noise. For this simulation, initial values were as follows: $A(0)$ = 0.06V, $f(0)$ = 90Hz, $\phi(0)$ = 2°, while the noise magnitudes were as follows: $\sigma_{e1} = 10^{-4}$, $\sigma_{e2} = 10^{-4}$, $\sigma_A = 10^{-3}$, $\sigma_f = 10^{-4}$ and $\sigma_\phi = 10^{-4}$. Note that a warmup period of approximately 500 samples was used to allow the filters to initialise, and this results in an offset from the initial value at the reported t = 0s in the plots shown below.

In [7], the simulations reflected single phase conditions. Accordingly, the random variations in frequency and phase difference were small, with maximum variations of 4e-2 Hz and 3e-1 degrees respectively, and no variation in signal amplitude. In the current simulation, as shown in Figure 3.1, the true frequency varies by approximately 10Hz, the phase difference by 6e-1 degrees, and the amplitude by about 4e-2 V, which is approximately ±50% of its mean value.

Results are presented here for the following methods:

- ANF and Hilbert for frequency tracking;
- DTFT (ANF based frequency) and Hilbert for phase difference tracking; and
- DTFT (ANF based frequency) and Hilbert for amplitude tracking.

Note these implementations are our own, but based on the literature cited above. Figure 3.2 - 3.4 show the tracking performance for frequency, phase difference and amplitude respectively. In each case the tracked values are shown in the upper graph, with the residual errors below. The frequency tracking errors are high bandwidth for the Hilbert method and low bandwidth for the ANF method. For phase difference, the Hilbert method shows good tracking with some time delay, while the DTFT results appear dominated by the frequency errors of the ANF upon which it relies. Similarly, for amplitude, the DTFT method shows large errors while the Hilbert method tracks relatively well with some time delay.

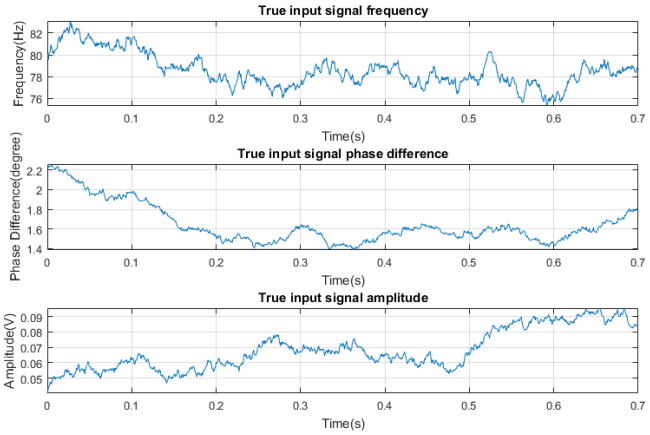

Fig. 3.1: Input signal's parameters

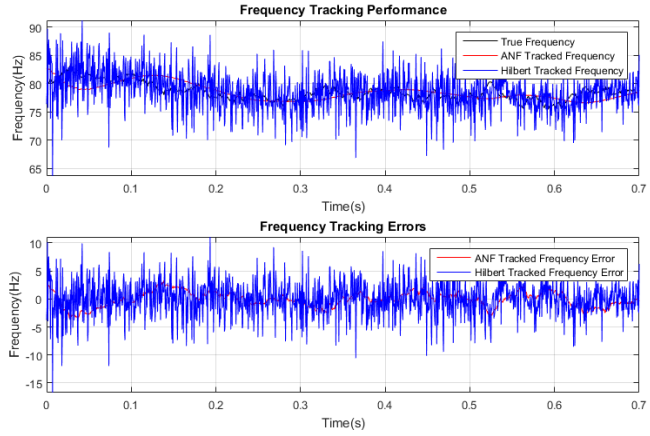

Fig. 3.2: Frequency tracking performance

In general terms, therefore, the rapidly changing errors for frequency tracking for the Hilbert method do not result in large amplitude and phase difference errors, while conversely, the slowly changing errors from the ANF method lead to poorer tracking for amplitude and phase when using DTFT. Table I shows the standard deviation for each method and parameter, and the Root Mean Squared Error (RMSE), calculated using:

$$RMSE = \sqrt{\frac{1}{n}\sum_{i=1}^{n}(\hat{Y}(n) - Y(n))^2} \qquad (27)$$

where $Y(n)$ and $\hat{Y}(n)$ are the true and estimated values.

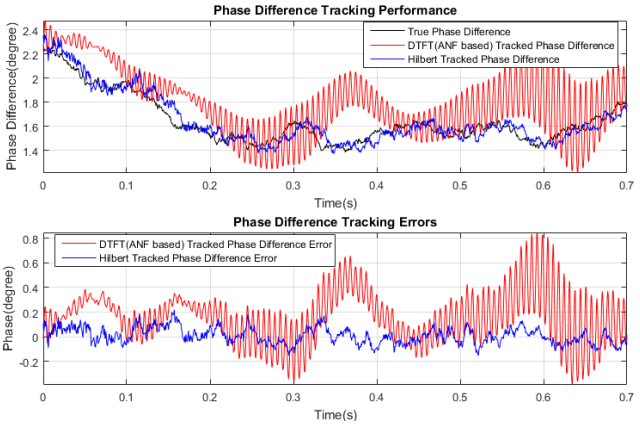

Fig. 3.3: Phase difference tracking performance

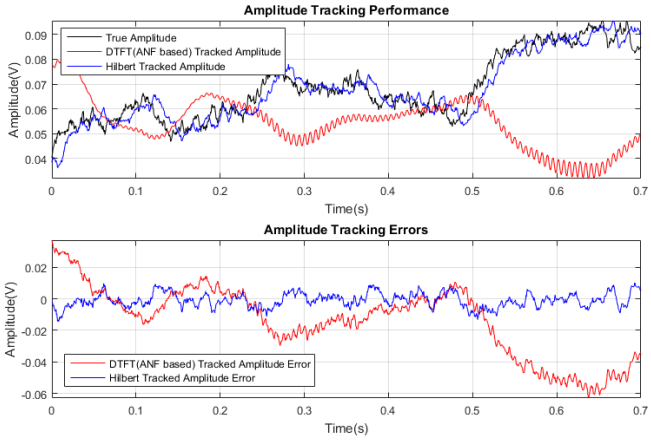

Fig. 3.4: Amplitude tracking performance

The std and RMSE result for frequency are broadly similar for the ANF and Hilbert methods. For phase difference and amplitude, the stds of the Hilbert method are 2-3 times smaller than those for the ANF/DTFT hybrid method. Similarly the RMSE for Hilbert is 3-6 times smaller.

TABLE I. QUANTIZED TRACKING PERFORMANCE

Method and Parameter	ANF	DTFT	Hilbert
Frequency RMSE (Hz)	1.0500e+1	N/A	1.0136e+1
Phase Difference RMSE (°)	N/A	1.2440e+0	2.1770e-1
Amplitude RMSE (V)	N/A	2.4073e-2	7.8850e-3
Frequency std (Hz)	1.0493e+1	N/A	1.0098e+1
Phase Difference std (°)	N/A	1.2389e+0	3.1670e-1
Amplitude std (V)	N/A	1.9967e-2	7.8304e-3

More generally, the advantages and disadvantages the various signal processing techniques discussed in this paper are summarized in Table II as follows:

TABLE II. ADVANTAGES AND DISADVANTAGES OF EACH METHOD

Method	Advantages	Disadvantages
Discrete Fourier Transform	Track all parameters simultaneously (using ANF for frequency tracking); computationally efficient in recursive algorithmic form.	Spectrum leakage; limited dynamic response; trade-off between time and frequency resolution.
Digital PLL	Tracks all parameters simultaneously; suppresses harmonic interference.	Limited dynamic response; result update once per cycle; limited tracking range.
Adaptive Notch Filter	Good ability to suppress noise.	Limited dynamic response; slow convergence; poor dealing with amplitude change; trade-off between convergence speed and precision.
Digital Correlation	Effectively removes random noise; computationally efficient.	Cannot suppress harmonic noise; result update once per cycle.
Hilbert Transform	Track all parameters simultaneously; computationally efficient; high precision tracking	Sensitive to random and harmonic noise; needs strict pre-filter; limited dynamic response

IV. CONCLUSION

With the increasing computation power available at low cost and with low power consumption, there are continuing opportunities to improve the signal processing techniques used for CMF metering. An important future area of CMF meter application is two-phase flow, where all of the measurement parameters are subject to large and rapid variations. Previous research into signal processing techniques has typically excluded consideration of these difficult conditions – specifically, it has commonly been assumed that the amplitude of the sensor signals is constant. This paper has discussed several current methods, and has evaluated their performance in a simulation of two-phase flow conditions, where frequency, amplitude and phase difference have all varied simultaneously.

Future work will extend the set of benchmark simulations, and develop new signal processing techniques suited to the challenging conditions of two-phase flow measurement.

REFERENCES

[1] T. Wang and R. Baker, "Coriolis flowmeters: a review of developments over the past 20 years, and an assessment of the state of the art and likely future directions," *Flow Meas. Instrum.*, vol. 40, pp. 99–123, Dec. 2014.

[2] M. Henry, "Self-validating digital Coriolis mass flow meter," *Comput. Control Eng. J.*, vol. 11, no. 5, pp. 219–227, Oct. 2000.

[3] M. Zamora and M. P. Henry, "An FPGA Implementation of a Digital Coriolis Mass Flow Metering Drive System," *IEEE Trans. Ind. Electron.*, vol. 55, no. 7, pp. 2820–2831, Jul. 2008.

[4] R. J. Reizner, "Coriolis - The almost perfect flow meter," *Comput. Control Eng. J.*, vol. 14, no. 4, pp. 28–33.

[5] J. Ruoff, W. Gauchel, and H. Kück, "Advances in Signal Acquisition and Signal Processing of Coriolis Flow Meters," *Procedia Eng.*, vol. 87, pp. 1585–1588, 2014.

[6] P. Yi, Y. Tu, M. Xie, and T. Shen, "Analysis of phase difference tracking methods for signal of coriolis mass flowmeter," in *Proceedings of the 10th World Congress on Intelligent Control and Automation*, 2012, pp. 4368–4373.

[7] Y. Tu, H. Yang, H. Zhang, and X. Liu, "CMF Signal Processing Method Based on Feedback Corrected ANF and Hilbert Transformation," *Meas. Sci. Rev.*, vol. 14, no. 1, 2014.

[8] A. Svete, J. Kutin, G. Bobovnik, and I. Bajsić, "Theoretical and experimental investigations of flow pulsation effects in Coriolis mass flowmeters," *J. Sound Vib.*, vol. 352, pp. 30–45, Sep. 2015.

[9] C. Clark and R. Cheesewright, "Experimental determination of the dynamic response of Coriolis mass flow meters," *Flow Meas. Instrum.*, vol. 17, no. 1, pp. 39–47, Mar. 2006.

[10] C. Clark, R. Cheesewright, S. Wang, M. Henry, M. Zamora, and M. Tombs, "A radically new dynamic response capability for Coriolis flow meters," *Sensors Actuators A Phys.*, vol. 123–124, pp. 54–62, Sep. 2005.

[11] C. Clark, R. Cheesewright, and S. Wang, "Prediction of the Dynamic Performance of Fast Response Coriolis Meter Systems," *IEEE Trans. Instrum. Meas.*, vol. 57, no. 1, pp. 95–99, Jan. 2008.

[12] M. P. Henry, C. Clark, M. Duta, R. Cheesewright, and M. Tombs, "Response of a Coriolis mass flow meter to step changes in flow rate," *Flow Meas. Instrum.*, vol. 14, no. 3, pp. 109–118, Jun. 2003.

[13] M. Tombs, M. Henry, F. Zhou, R. M. Lansangan, and M. Reese, "High precision Coriolis mass flow measurement applied to small volume proving," *Flow Meas. Instrum.*, vol. 17, no. 6, pp. 371–382, Dec. 2006.

[14] M. Henry, M. Tombs, M. Zamora, and F. Zhou, "Coriolis mass flow metering for three-phase flow: A case study," *Flow Meas. Instrum.*, vol. 30, pp. 112–122, Apr. 2013.

[15] H. Kitami and H. Shimada, "Signal processing method, signal processing apparatus, and coriolis flowmeter," U.S. Patent 8676517, 18-Mar-2014.

[16] Y. Tu and H. Zhang, "Method for CMF Signal Processing Based on the Recursive DTFT Algorithm With Negative Frequency Contribution," *IEEE Trans. Instrum. Meas.*, vol. 57, no. 11, pp. 2647–2654, Nov. 2008.

[17] T. Shen, Y. Tu, and H. Zhang, "A novel time varying signal processing method for Coriolis mass flowmeter.," *Rev. Sci. Instrum.*, vol. 85, no. 6, p. 065116, Jun. 2014.

[18] H. Wen, J. Zhang, Z. Meng, S. Guo, F. Li, and Y. Yang, "Harmonic Estimation Using Symmetrical Interpolation FFT Based on Triangular Self-Convolution Window," *IEEE Trans. Ind. Informatics*, vol. 11, no. 1, pp. 16–26, Feb. 2015.

[19] T. Shen, Y. Tu, M. Li, and H. Zhang, "A new phase difference measurement algorithm for extreme frequency signals based on discrete time Fourier transform with negative frequency contribution.," *Rev. Sci. Instrum.*, vol. 86, no. 1, p. 015104, Jan. 2015.

[20] Y. Tu, T. Shen, H. Zhang, and M. Li, "Two New Sliding DTFT Algorithms for Phase Difference Measurement Based on a New Kind of Windows," *Meas. Sci. Rev.*, vol. 14, no. 6, pp. 350–356, Jan. 2014.

[21] B. S. Freeman, "Digital phase locked loop signal processing for coriolis mass flow meter," U.S. Patent 5804741, 08-Sep-1998.

[22] H. V. Derby, T. Bose, and S. Rajan, "Method and apparatus for adaptive line enhancement in Coriolis mass flow meter measurement," U.S. Patent 5555190, 10-Sep-1996.

[23] H. Y. Yang, Y. Q. Tu, and H. T. Zhang, "A Frequency Tracking Method Based on Improved Adaptive Notch Filter for Coriolis Mass Flowmeter," *Appl. Mech. Mater.*, vol. 128–129, pp. 450–456, Oct. 2011.

[24] Wei Ni and Kejun Xu, "An improved signal processing method for Coriolis mass flowmeter based on time-varying signal model," in *Fifth World Congress on Intelligent Control and Automation (IEEE Cat. No.04EX788)*, 2004, vol. 4, pp. 3787–3790.

[25] G. Yin, L. Guo, and X. Li, "An Amplitude Adaptive Notch Filter for Grid Signal Processing," *IEEE Trans. Power Electron.*, vol. 28, no. 6, pp. 2638–2641, Jun. 2013.

[26] T. Wray, "Coriolis flow meter with adjustable excitation phase," U.S. Patent 6332366, 25-Dec-2001.

[27] G. R. Duffill, S. M. Jones, and A. T. Patten, "Meter electronics and methods for determining a liquid flow fraction in a gas flow material," U.S. Patent 7974792, 05-Jul-2011.